Accepted Manuscript

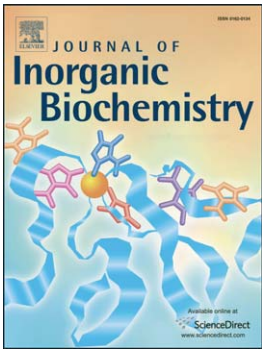

$[(\eta^6$-*p*-cymene)$Ru(H_2O)_3]^{2+}$ binding capability of aminohydroxamates – A solution and Solid state study

Péter László Parajdi-Losonczi, Attila Csaba Bényei, Éva Kováts, István Timári, Tereza Radosova Muchova, Vojtech Novohradsky, Jana Kasparkova, Péter Buglyó

PII: S0162-0134(16)30058-7
DOI: doi: 10.1016/j.jinorgbio.2016.02.032
Reference: JIB 9946

To appear in: *Journal of Inorganic Biochemistry*

Received date: 29 September 2015
Revised date: 11 February 2016
Accepted date: 25 February 2016

Please cite this article as: Péter László Parajdi-Losonczi, Attila Csaba Bényei, Éva Kováts, István Timári, Tereza Radosova Muchova, Vojtech Novohradsky, Jana Kasparkova, Péter Buglyó, $[(\eta^6$-*p*-cymene)$Ru(H_2O)_3]^{2+}$ binding capability of aminohydroxamates – A solution and Solid state study, *Journal of Inorganic Biochemistry* (2016), doi: 10.1016/j.jinorgbio.2016.02.032

$[(\eta^6\text{-}p\text{-cymene})Ru(H_2O)_3]^{2+}$ Binding Capability of Aminohydroxamates – A Solution and Solid State Study

Péter László Parajdi-Losonczi [a], Attila Csaba Bényei [b], Éva Kováts [c], István Timári [a], Tereza Radosova Muchova [d] , Vojtech Novohradsky [e], Jana Kasparkova [d,e], Péter Buglyó [a,*]

[a] Department of Inorganic and Analytical Chemistry, University of Debrecen, H-4010 Debrecen, P.O.Box 21, Hungary.
[b] Department of Physical Chemistry, University of Debrecen, H-4010 Debrecen P.O.Box 7, Hungary.
[c] HAS Wigner Research Centre for Physics, 1121 Budapest, Konkoly Thege Miklós u. 29-33, Hungary.
[d] Department of Biophysics, Faculty of Science, Palacky University, 17. Listopadu 12, 77146 Olomouc, Czech Republic.
[e] Institute of Biophysics, Academy of Sciences v.v.i. of the Czceh Republic, Kralovopolska 135, 615 65 Brno, Czech Republic.

Abstract

Complex forming capabilities of $[(\eta^6\text{-}p\text{-cymene})Ru(H_2O)_3]^{2+}$ with aminohydroxamates (2-amino-N-hydroxyacetamide (α-alahaH), 3-amino-N-hydroxypropanamide (β-alahaH) and 4-amino-N-hydroxybutanamide (γ-abhaH)) having the primary amino group in different chelatable position to the hydroxamic function were studied by pH-potentiometry, NMR and MS methods. Formation of stable [O,O] and mixed [O,O][N,N] chelated mono- and dinuclear species is detected in partially slow with α-alahaH and β-alahaH or in fast processes with γ-abhaH and the formation constants of the complexes present in aqueous solution are reported. Synthesis, spectral (NMR, IR) and ESI mass spectrometric characterization of novel dinuclear α-alaninehydroximato complexes containing the half-sandwich type Ru(II) core is described. The crystal and molecular structure of $[\{(\eta^6\text{-}p\text{-cymene})Ru\}_2(\mu^2\text{-}\alpha\text{-alahaH}_{-1})(H_2O)Br]Br\cdot H_2O$ (**1**) and $[\{(\eta^6\text{-}p\text{-cymene})Ru\}_2(\mu^2\text{-}\alpha\text{-alahaH}_{-1})(H_2O)Cl]BF_4\cdot H_2O$ (**2**) was determined by single crystal X-ray diffraction method. In the complexes one half-sandwich core is coordinated by a hydroxamate [O,O] chelate while the other one by $[N_{amino},N_{hydroxamate}]$ fashion of the bridging ligand. In both cases the remaining coordination sites of one of the Ru cores are taken by a halide ion whiles the other one by a water molecule. Reaction of **2** with 9-methylguanine indicates the N7 coordination of this simple DNA model. Complexes **1** and **2** were tested for their *in vitro* cytotoxicity using human-derived cancer cell lines (A2780, MCF-7, SKOV-3, HCT116, HeLa) and showed no anti-proliferative activity in the micromolar concentration range.

* Corresponding author: buglyo@science.unideb.hu, phone number: + 36 52 512900/22305.

1. Introduction

Hydroxamic acids with the general formula of $R_1(CO)N(R_2)OH$ are important class of biomolecules and are attracting an increasing attention. They are known, for example, as constituents of siderophores and enhance the uptake of various metal ions (e.g. Fe^{3+}) in microorganisms.[1-3] Hydroxamates are also considered as effective inhibitors of various metalloenzymes.[3-4] Both type of biological activity is obviously connected to their capability of forming stable five-membered [O,O] chelate(s) with various, mostly hard type metal ions. Based on the inhibition of a Zn(II)-containing metalloenzyme, histone deacetylase, a monohydroxamic acid, suberoylhydroxamic acid (SAHA), is currently undergoing clinical use as a treatment for cutaneous T-cell lymphoma.[5]

Half-sandwich type Ru(II) complexes with promising anti-proliferative properties are also in the focus of intensive research in recent decades. Earlier studies mostly dealt with the design, synthesis, characterization and biological test of these $[(\eta^6\text{-arene})Ru(XY)Z]$ type (arene = benzene(derivative), XY = chelating, Z = monodentate ligand) complexes.[6-10] Recent years research focusing on their solution behaviour or the interaction with various high[11-17] or low molecular mass[18-29] biomolecules is also in progress.

Lately we have combined hydroxamates and half-sandwich $[(\eta^6\text{-}p\text{-cym})M]^{2+}$ (*p*-cym = *p*-cymene = 1-methyl-4-(1-methylethyl)benzene; M = Ru, Os) entities, both having potential biological activity, into one molecule hoping to obtain compounds with beneficial features.[18,30] Although detailed solution equilibrium studies revealed that monohydroxamates are capable of binding $[(\eta^6\text{-}p\text{-cym})Ru(H_2O)_3]^{2+}$ in stable complexes over a wide pH-range in aqueous solution, biological tests on human-derived ovarian cancer cell lines (A2780 and A2780 cisR) indicated no improved biological activity. The lack of antiproliferative activity of these compounds was interpreted in terms of labile behaviour of the [O,O] chelate formed despite the high thermodynamic stability of the complexes.[18]

Presence of $Ru\text{-}N_{amino}$ bond(s) in $[(\eta^6\text{-arene})Ru(XY)Z]$ complexes seems to result in more inert behaviour.[31] Hydroxamate derivatives of simple amino acids also bear a primary amino group beside the hydroxamic function therefore may represent ligands with beneficial binding properties for $[(\eta^6\text{-}p\text{-cym})Ru(H_2O)_3]^{2+}$ in terms of the appropriate kinetic inertness. Aminohydroxamates have been shown to act as exclusive [O,O] chelators for hard metal ions (Fe^{3+}, Al^{3+}) but soft metal ions were found to have a preference for [N,N] coordination in the basic pH-range with the involvement of the hydroxamate-N of primary hydroxamates in metal ion binding.[32-37] For borderline metal ions (e.g. Cu^{2+}) the formation of stable pentanuclear

metallacrowns with the parallel coodination of both types of the donor sets of α– or β–aminohydroxymates was detected both in solution and in the solid state.[38-39]

In the present work, we sought to gain a deeper insight into the effect of the presence of the terminal amino group beside the hydroxamate function on the $[(\eta^6\text{-}p\text{-cym})Ru(H_2O)_3]^{2+}$ ion binding in solution and its role on the stability, stoichiometry, nuclearity and binding architecture of the half-sandwich type Ru(II) aminohydroxamate complexes.

Herein we report on the results of a solution equilibrium study relating the interaction of $[(\eta^6\text{-}p\text{-cym})Ru(H_2O)_3]^{2+}$ with 2-amino-N-hydroxyacetamide (α-alahaH), 3-amino-N-hydroxypropanamide (β-alahaH) and 4-amino-N-hydroxybutanamide (γ-abhaH) (Fig. 1) obtained by the combined use of pH-potentiometry, NMR and ESI-MS together with the synthesis, characterization, biological test and 9-methylguanine (as a simple DNA model) binding capabilities of $[\{(\eta^6\text{-}p\text{-cym})Ru\}_2(\mu^2\text{-}\alpha\text{-alahaH}_{-1})(H_2O)Br]Br\cdot H_2O$ (**1**) and $[\{(\eta^6\text{-}p\text{-cym})Ru\}_2(\mu^2\text{-}\alpha\text{-alahaH}_{-1})(H_2O)Cl]BF_4\cdot H_2O$ (**2**) complexes.

2. Experimental

Materials and methods

$RuCl_3\cdot xH_2O$, α-terpinene, $AgNO_3$, O-benzylhydroxylamine hydrochloride, N-carbobenzyloxy-γ-aminobutanoic acid, ethylchloroformate, N-methylmorpholine, Pd/C (10 %), KBr and $NaBF_4$, 9-methylguanine of highest purity were all commercial products (Merck, Aldrich, and Reanal) and used as received. CH_3OH, CH_2Cl_2 and THF, used for the preparation of the ligands, were purchased from Molar chemicals. Hydroxylamine hydrochloride was purified by recrystallization.[40] α-AlahaH and β-alahaH·HCl were synthesized using a published method.[41] $[(\eta^6\text{-}p\text{-cym})RuCl_2]_2$ was synthesized and purified according to a literature procedure.[42] Aqueous solution of $[(\eta^6\text{-}p\text{-cym})Ru(H_2O)_3](NO_3)_2$ was obtained from $[(\eta^6\text{-}p\text{-cym})RuCl_2]_2$ by the removal of chloride ion using equivalent amount of silver nitrate. ^{1}H NMR spectra were recorded on a Bruker Avance 360 or 400 NMR spectrometer at room temperature in D_2O or $CDCl_3$ and referenced to 3-(trimethylsilyl)-1-propanesulfonic acid sodium salt (TSP) or to the ^{1}H resonances of the residual solvents. ESI-TOF MS measurements in the positive mode were carried out on a Bruker micrOTOF-Q instrument. IR spectra as KBr pellets were recorded on a Perkin Elmer FTIR Paragon 1000 PC instrument. Elemental analyses were conducted on Elementar Vario MICRO CUBE instrument at the Department of Organic Chemistry, University of Debrecen, Hungary.

Crystal structure analysis

Diffraction intensity data collection was carried out at 100 K on a SuperNova diffractometer equipped with an Atlas detector using Cu-*K*α radiation (λ = 1.5418 Å). The structure was solved by SIR-92 program[43] in centrosymmetric space group P-1 (No.2) as it is usually expected for a racemic compound and refined by full-matrix least-squares method on F^2. Non-hydrogen atoms were refined anisotropically using the SHELX package[44] except one fluorine of the tetrafluoroborate anion in structure **2**. Publication material was prepared with the WINGX- suite[45] and publCIF[46]. In structure **2** the BF_4^- counter ion and the methyl groups of the *i*-Pr moiety of one of the *p*-cymene ligands are disordered over two positions with occupancy of ca. 68:32 ratio. Hydrogen atoms were treated with a mixture of independent and constrained refinement. C-H and N-H hydrogen atoms were placed into geometric position and methyl groups were refined using a riding model. Hydrogen atoms of water molecules were found at the difference electron density map but the distances of hydrogen and oxygen atoms should be restrained in the final stage of the refinement. Still the orientation of water molecules is ambiguous but presence of heavy atoms prevents more exact determination of place of hydrogen atoms and orientation of water molecules. This ambiguities resulted B and C level errors in donor-hydrogen distances, as detected by the checkcif facility, but they do not influence the overall correctness of the structures. Crystallographic and experimental details are summarized in Table 1. The remaining peaks at the difference electron density maps are located close to the ruthenium atoms. All the crystallographic data for **1** and **2** are deposited in the Cambridge Crystallographic Data Centre under CCDC 1423422-1423423.

Preparation of the ligands and complexes

Benzyl(N-carbobenzyloxy)-γ-aminobutanehydroxamate

O-benzylhydroxylamine hydrochloride (4.07 g, 25 mmol) was dissolved in dry methanol (40 ml) and chilled in an ice-bath under nitrogen. KOH (1.4 g, 25 mmol) as pellets, was added to the solution and the mixture was stirred in ice-bath for 10 min meanwhile solid KCl formed. In another flask N-carbobenzyloxy-γ-aminobutanoic acid (4.0 g, 17 mmol) was dissolved in dry THF (50 ml) under nitrogen and cooled to 0 °C in ice-bath. Ethylchloroformate (2.0 ml, 21 mmol) followed by N-methylmorpholine (2.4 ml, 22 mmol) were added while stirring. The reaction mixture was stirred for 40 min under inert conditions, white precipitate (N-

methylmorpholinium chloride) formed. The free O-benzylhydroxylamine solution was filtered into a three-neck flask while the solution of the mixed anhydride filtered into a dropping funnel. The latter solution was added dropwise to the former within 5 min while stirring under nitrogen at 0 °C. The resulting reaction mixture was stirred overnight under nitrogen at room temperature. Next day the solvent was evaporated from the milky-like reaction mixture and the remaining solid was dissolved in CH_2Cl_2 (100 ml). It was extracted with 0.5 M aqueous citric acid solution (3x30 ml) and saturated $NaHCO_3$ solution (2x25 ml). The extract was washed with 25 ml water, then dried on $MgSO_4$ and evaporated in vacuo. The pure product was obtained as a white solid after recrystallization from 30 ml ethyl acetate. Yield: 4.31 g (75 %). ^{1}H NMR (360 MHz, $CDCl_3$, 298 K): δ = 1.81 m [-*CH*$_2$]; 2.08 m [-*CH*$_2$]; 3.20 m [-*CH*$_2$]; 4.93 s [-*CH*$_2$]; 5.07 s [-*CH*$_2$]; 7.34 m [Ar (-*H*)].

4-amino-N-hydroxybutanamide hydrochloride (γ-abhaH·HCl)

In a two-neck flask benzyl(N-carbobenzyloxy)-γ-aminobutanehydroxamate (1.0 g, 2.9 mmol) was dissolved in dry ethyl acetate (35 ml) under nitrogen. Pd/C (10 %, 0.20 g) and methanolic solution of HCl (2.6 M, 1.12 ml) was added and the suspension was stirred under H_2 atmosphere at room temperature. After 4.5 h the catalyst was filtered off and washed with methanol (3x15 ml). The resulting solution was evaporated and the oily product was dried in vacuo. Yield: 0.39 g (87 %). ^{1}H NMR (360 MHz, D_2O, 298 K): δ = 1.93 m [-*CH*$_2$]; 2.26 t [-*CH*$_2$]; 3.00 t [-*CH*$_2$].

[{(η^6-p-cym)Ru}$_2$(μ^2-α-alahaH$_{-1}$)(H$_2$O)Br]Br·H$_2$O (**1**)

[(η^6-*p*-cym)$RuCl_2$]$_2$ (61.16 mg, 0.09987 mmol) and α-alahaH (11.79 mg, 0.1010 mmol) was dissolved in water (2 ml) and stirred for 1 h. The pH of the solution was set to pH ~ 5 with a few drops of concentrated fresh carbonate-free NaOH solution and stirred for another 2 h. The resulting red solution was filtered off and KBr (48.70 mg, 0.4092 mmol) was added. On cooling to 4 ^{o}C, the red crystalline solid was separated which was filtered, washed with dry diethyl ether and dried in vacuum. Yield: 42.20 mg (55 %). Calcd. for $C_{23}H_{38}N_2O_4Ru_2Br_2$: C, 35.95; H, 4.98; N, 3.65; found C, 35.69; H, 5.08; N, 3.67. ^{1}H NMR (400 MHz, D_2O, 298 K): δ = 1.25 m [12H, -CH(*CH*$_3$)$_2$ (*p*-cym)] and [3H, -*CH*$_3$ (α-Alaha)]; 2.21 s, 2.23 s [6H, -*CH*$_3$ (*p*-cym)]; 2.77 m, 2.85 m [2H, -*CH*$(CH_3)_2$ (*p*-cym)]; 3.38 m [1H, -*CH* (α-Alaha)]; 5.47 d, 5.53 d, 5.69 d, 5.74 d, 5.55 m, 5.64 m, 5.78 m [8H, Ar(-*H*)]. IR (KBr): ν_{max}/cm^{-1} = 3380 br (O-H),

2961 s (C-H), 2927 s (C-H), 2871 s (C-H), 1578 s (C=O). MS (ESI-TOF): m/z = 652.983 $[((\eta^6\text{-}p\text{-cym})Ru)_2(\alpha\text{-alahaH}_{-1})(Br)]^+$ (simulated = 652.989).

[{(η^6-p-cym)Ru}$_2$(μ^2-α-alahaH$_{-1}$)(H_2O)Cl]BF_4·H_2O (**2**)

$[(\eta^6\text{-}p\text{-cym})RuCl_2]_2$ (61.20 mg, 0.09994 mmol) and α-alahaH (11.70 mg, 0.1002 mmol) was dissolved in water (3 ml) and stirred for 1 h. The pH of the solution was set to pH ~ 5 with a few drops of concentrated fresh carbonate-free NaOH solution and stirred for 90 min. The resulting red solution was filtered and $NaBF_4$ (22.00 mg, 0.2004 mmol) was added. The solution was then cooled to 4 ^oC, the red crystalline complex obtained was filtered, washed with dry diethyl ether and dried in vacuum for 10 min. Yield: 38.29 mg (52 %). Calcd. for $C_{23}H_{38}N_2O_4Ru_2ClBF_4$: C, 37.79; H, 5.24; N, 3.83; found C, 37.67; H, 5.36; N, 3.87. ^{1}H NMR (360 MHz, D_2O, 298 K, TSP): δ = 1.25 m [12H, -CH*(CH_3)$_2$* (*p*-cym)] and [3H, -*CH_3* (α-Alaha)]; 2.21 s [6H, -*CH_3* (*p*-cym)]; 2.80 m [2H, -*CH*(CH_3)$_2$ (*p*-cym)]; 3.38 m [1H, -*CH* (α-Alaha)]; 5.45 d, 5.52 d, 5.56 d, 5.63 d, 5.67 d, 5.73 d, 5.78 d, 5.83 d [8H, Ar(-*H*)]. IR (KBr): ν_{max}/cm^{-1} = 3384 br (O-H), 2963 s (C-H), 2930 s (C-H), 2873 s (C-H), 1578 s (C=O), 1060 br (B-F). MS (ESI-TOF): m/z = 609.040 $[((\eta^6\text{-}p\text{-cym})Ru)_2(\alpha\text{-alahaH}_{-1})(Cl)]^+$ (simulated = 609.040).

Solution studies

For solution studies doubly deionised and ultra-filtered water was obtained from a Milli-Q RG (Millipore) water purification system. pH-potentiometric measurements were carried out at an ionic strength of 0.20 M KCl and at 25.0 ± 0.1 ºC. Carbonate-free KOH solutions of known concentrations (*ca.* 0.2 M) were used as titrant. HCl stock solutions were prepared from concentrated HCl and their concentrations were determined by potentiometric titrations using the Gran's method.[47] A Mettler Toledo DL50 titrator equipped with a DGi 114-SC electrode was used for the pH-metric measurements. The electrode system was calibrated according to Irving *et al.*,[48] the pH-metric readings could therefore be converted into hydrogen ion concentration. The water ionization constant, pK_w, was 13.75 ± 0.01 under the conditions employed. Titrations were performed in the pH range 2.0 – 11.0. Initial volume of the samples was 15.00 ml. The metal ion concentrations were varied in the range 1.0 – 3.5 mM and 1:1, 1:2 and 2:1 metal to ligand ratios were titrated. For the metal ion containing systems a maximum waiting time of 15 minutes was applied. The reproducibility of the equilibrium titration points included in the evaluation was within 0.005 pH unit. The samples

were in all cases completely deoxygenated by bubbling purified argon for *ca*. 15 min prior the measurements. Calculation of the stability constants ($\beta_{p,q,r} = [Ru_pA_qH_r]/[Ru]^p[A]^q[H]^r$; where "Ru" stands for $[(\eta^6\text{-}p\text{-cym})Ru]^{2+}$ and "A" represents the deprotonated forms of the aminohydroxamic acids) of the complexes using the titration curves was attempted by the PSEQUAD or SUPERQUAD computer programs.[49-50] During the calculations hydrolysis of $[(\eta^6\text{-}p\text{-cym})Ru(H_2O)_3]^{2+}$ and its interaction with chloride ion were taken into consideration and the following species was assumed: $[\{(\eta^6\text{-}p\text{-cym})Ru\}_2(\mu^2\text{-}OH)_2]^{2+}$ ($\log\beta_{2,0,-2} = -7.12$), $[\{(\eta^6\text{-}p\text{-cym})Ru\}_2(\mu^2\text{-}OH)_3]^{+}$ ($\log\beta_{2,0,-3} = -11.88$).[18]

^{1}H NMR titrations were carried out on a Bruker Avance 360 or 400 NMR instrument at 278 K in the presence of 0.20 M KNO_3. Chemical shifts are reported in ppm (δ_H) from sodium 3-(trimethylsilyl)-propionate (TSP) as internal reference. Titrations were carried out in D_2O (99.8 %) at c_{Ru} = 0.01 M in order to register the pH dependence of the chemical shifts of the nuclei of hexahapto bonded *p*-cymene. pH was set up with NaOD or DNO_3 in D_2O. Individual samples were equilibrated at least for 1 h prior measurements. pH* values (direct pH-meter readings in a D_2O solution of a pH-meter calibrated in H_2O according to Irving *et al*.[48]) were converted to pH values measureable at an ionic strength of 0.20 M using the following equation: pH = pH* + 0.40. The interaction of **2** with 9-methylguanine was monitored in D_2O using 1:1 and 1:2 molar ratios at 298 K adopting the method in Ref. [51].

For the ESI-MS analysis of the solutions the measurements were performed in water at 0.4 mM $[(\eta^6\text{-}p\text{-cym})Ru(H_2O)_3]^{2+}$ concentration at different pH values and at 1:1 metal ion to ligand ratio. Temperature of drying gas (N_2) was 180°C. The pressure of the nebulizing gas (N_2) was 0.3 bar. The flow rate was 3 μl/min. The spectra were accumulated and recorded by a digitalizer at a sampling rate of 2 GHz. DataAnalysis (version 3.4) was used for the calculations.

Cytotoxicity tests

The human ovarian carcinoma A2780, the human breast cancer MCF-7 and human ovarian adenocarcinoma SKOV-3 cells were kindly supplied by Professor B. Keppler, University of Vienna (Austria). The human colon carcinoma HCT116 cells were a kind gift of Dr. M. Brazdova, Institute of Biophysics, Brno (Czech Republic), the human cervix adenocarcinoma HeLa cells were obatined from ATCC (Manassas, Virginia, U.S.). The A2780 cells were grown in RPMI 1640 medium (PAA; Pasching, Austria) supplemented with streptomycin

(100 μg mL^{-1}), penicillin (100 U mL^{-1}) (both Sigma, Prague, Czech Republic) and 10% heat inactivated fetal bovine serum (PAA; Pasching, Austria). The MCF-7, HeLa, SKOV-3 and HCT-116 cells were grown in DMEM medium (PAA; Pasching, Austria) supplemented with gentamycin (50 μg mL^{-1}, Serva, Heidelberg, Germany) and 10% heat inactivated fetal bovine serum (PAA; Pasching, Austria). The cells were cultured in a humidified incubator at 37 °C in a 5% CO_2 atmosphere and subcultured 2-3 times a week with an appropriate plating density. Cytotoxic effect of compounds **1** and **2** were evaluated by using assays based on the neutral red (NR) uptake. The adherent cells were plated out 20 h prior to testing in 96-well tissue culture plates at a density of 10^4 cells/well (A2780) or 4 x 10^3 cells/well (MCF-7, HeLa, SKOV-3 and HCT-116) in 100 μL of medium. The cells were treated for 72 h with the compounds at the final concentrations in the range of 0 to 0.5 mM in a final volume of 200 μL/well. Concentrations of the compounds in the medium during the treatment were verified by flameless atomic absorption spectrometry. Thereafter, a viability of the cells was tested by NR assay as described previously.[52] Briefly, after the treatment period, 20 μL of a 0.33% solution of NR in phosphate buffered saline (PBS) was added to each well with adherent cells and the plate was incubated at 37 °C in a humidified 5% CO_2 atmosphere for 2 h. Afterwards, the dye containing medium was carefully removed and the cells were quickly rinsed with PBS. The incorporated dye was then solubilized in 200 μL of 1% acetic acid in 50% ethanol, allowed to stand for 10 min at room temperature and the absorbance was measured at λ = 540 nm with absorbance reader Synergy MX (Biotek,VT, USA). The background absorbance of the plates at 690 nm was also measured and subtracted from 540 nm measurement. The reading values were converted to the percentage of the control (percentage cell survival). All experiments were repeated at least three times, each repetition made in triplicate.

3. Results and discussion

3.1. Synthesis and characterization of the ligands

α–alahaH and β–alahaH·HCl were synthesized according to published procedures [41] while in the case of γ-abhaH·HCl a slightly modified synthetic route was used. For the α and β derivative the ligands were obtained from the appropriate methylesters and hydroxylamine followed by conversion to β–alahaH·HCl in the latter case. Pure products were obtained by recrystallization from ethanol and checked by NMR exhibiting the expected resonances. For γ–abhaH the Z-protected aminobutyric acid was activated with ethylchloroformate and the

mixed acid anhydride was reacted with O-benzyl-hydroxylamine. The doubly protected intermediate was subjected to hydrogenolysis affording the pure product as colourless oil.

3.2. Potentiometric results

To check the purity and the exact concentration of the aqueous solutions of the aminohydroxamate ligands pH-potentiometric measurements were carried out. As a representative example titration curve of α–alahaH is shown in Fig. 2a. The redetermined stepwise protonation constants of the ligands are summarized in Table 2 and are in excellent agreement (within 0.05 log units) with the previous data estimated under identical experimental conditions.[53-55]

Representative titration curves for the $[(\eta^6\text{-}p\text{-cym})Ru(H_2O)_3]^{2+}$ – ligand systems are shown in Fig. 2. For α- and β-alahaH slow complex formation processes were observed in the range 3.0 < pH < 7.0 and 4.5 < pH < 7.0, respectively, the usual waiting time (see Experimental) was not enough to reach complete pH equilibrium. This is also reflected in the shape of the titration curves. At the same time, for the $[(\eta^6\text{-}p\text{-cym})Ru(H_2O)_3]^{2+}$-γ–abhaH system fast processes were detected resulting in reliable and reproducible titration curves (Fig. 2c). Despite the above facts, analysis and comparison of the sets of titration curves may provide with valuable information. For the α-alahaH system at 2:1 metal ion to ligand ratio the three equivalents of base consumption is consistent with the formation of $[Ru_2AH_{-1}]^{2+}$ (Ru = $[(\eta^6\text{-}p\text{-cym})Ru]$) in which the second metal ion is coordinated via the [N,N] donor set of the ligand. This is also supported by the half amount of extra base consumption at 1:1 ratio by pH 5.5. For the β-alahaH system similar trend is observed, however, the formation of $[Ru_2AH_{-1}]^{2+}$ is accompanied by a separate step on the curve above pH ~ 4.5 suggesting smaller stability of this complex than that formed with α-alahaH. For γ–abhaH the titration curve at 2:1 ratio is more complex but still indicates the formation of a $[Ru_2A]$ type species.

The titration curves for all the systems can be fitted well with the models and complexes summarized in Table 2 while the calculated concentration distribution curves appear in Fig. 3. During model selection $[RuAH_{-1}]$ could be replaced by its dimeric form, $[Ru_2A_2H_{-2}]$. It is important to emphasize that for the $[(\eta^6\text{-}p\text{-cym})Ru(H_2O)_3]^{2+}$-γ–abhaH system, where stable pH-metric readings were available, reliable stability constants could be calculated for the complexes while in the case of the α– and β–alahaH the logβ values (shown by italic numbers in Table 2) should be treated as tentative only. Nevertheless, comparison of the stability constants in Table 2 allows to draw some useful conclusions too.

In all the three systems the complex formation starts with $[RuAH]^{2+}$ in which the ligands coordinate via a hydroxamate [O,O] chelate to the metal ion while the amino groups are protonated (see **I** in Fig. 4 (where, as representative examples, the suggested binding modes with γ-abhaH are shown)). [N,N] coordination mode with protonated hydroxamic function would mean $[RuA]^{+}$ stoichiometry. Furthermore the log*K** values of the three complexes with the various ligands (Table 2) referring to the (1) equilibrium process are well comparable with each other indicating identical strengths of the coordinating donor atom sets supporting thus the hydroxamate coordination mode.

$$Ru^{2+} + H_2A^{+} = [RuAH]^{2+} + H^{+} \quad (1)$$

With increasing pH slow complex formation processes were detected in the systems containing the α- and β-alahaH, but not with γ–abhaH ligand. Speciation curves (Fig. 3 A-C) indicate the binding of a second metal ion in each system resulting in the formation of $[Ru_2AH_{-1}]^{2+}$ in agreement with the three equivalents of base consumptions in the titration curves of each ligand at 2:1 metal ion to ligand ratio. This complex stoichiometry can be rationalized with the deprotonation of the hydroxamate-NH and the ammonium group as it is illustrated by **II** in Fig. 4. Although the $\log\beta_{Ru_2AH_{-1}}$ values can only be considered as tentative for the α- and β-alahaH ligand, the decreasing trend in the α → γ direction clearly supports the decreased stability of the [N,N] chelated species due to the increasing chelate size. Parallel with the formation of $[Ru_2AH_{-1}]^{2+}$, further increase in pH results in the displacement of the hydroxamate [O,O] coordinated metal ion with the formation of $[RuA]^{+}$. In principle, in the $[RuA]^{+}$ species the ligands can coordinate by [O,O] fashion with deprotonation of the water molecule at the third coordination site, however, the rather low pK_{RuAH} values, especially for the α and β derivative (Table 2), seem not to support this binding mode. It is more likely that these values belong to the metal ion assisted deprotonation and coordination of the ammonium group, resulting in the formation of **III** (Fig. 4) as the most plausible solution structure, but the formation of $[Ru_2A_2]^{2+}$ with $[(O,O)(NH_2)]$ coordination mode of the ligands can not be ruled out either. In all systems further deprotonation yields $[RuAH_{-1}]_x$ (x = 1-2) species that are indistinguishable by pH-potentiometry from each other. $[RuAH_{-1}]$ may be a mixed hydroxido complex (**IV**, Fig. 4), but ESI MS results also support the formation of the appropriate dinuclear complexes, $[Ru_2A_2H_{-2}]$ (*vide infra*). These species may consist of two [N,N] coordinated entities bridged by the hydroxamate oxygens of the ligands (**V**, Fig. 4).

3.2. ESI-TOF-MS results

ESI-TOF-MS measurements also provided valuable information in the identification of the species present in solution. As a representative example MS spectrum acquired in the $[(\eta^6\text{-}p\text{-cym})Ru(H_2O)_3]^{2+}$–γ–abhaH system at 1:1 ratio is shown in Fig. 5. Fig. 5 reveals that $[RuA]^+$ and $[Ru_2(AH_{-1})Cl]^+$ are the major complexes at pH = 6.07 supporting thus the pH-potentiometric results. The identified species existing at various ratios and pH values are summarized in Table 3 while, as a representative example, the estimated and observed isotope pattern for $[Ru_2A_2H_{-2}] + K^+$ in the γ–abhaH system can be seen in Fig. S2. For all the species in Table 3 the correct isotopic pattern was found proving in this way the identity of the complexes.

3.3. NMR results

Complex formation was also monitored by ^{1}H NMR spectroscopy. As a representative example, pH-dependence of the aromatic part of the spectra recorded in the $[(\eta^6\text{-}p\text{-cym})Ru(H_2O)_3]^{2+}$– γ–abhaH system at 1:1 metal ion to ligand ratio are shown in Fig. 6. At pH = 2.78 beside the doublets of the *p*-cymene ring hydrogens belonging to $[(\eta^6\text{-}p\text{-cym})Ru(H_2O)_3]^{2+}$ (5.73 and 5.98 ppm) and $[(\eta^6\text{-}p\text{-cym})Ru(H_2O)_2Cl]^+$ (5.63 and 5.85 ppm) species[20], a new pair of doublets also appears corresponding most likely to $[RuAH]^{2+}$. In accordance with the speciation in Fig. 3c at pH ~ 5 this becomes the predominant complex. On increasing the pH, small upfield shift of the resonances of $[RuAH]^{2+}$ is consistent with a slight change in the coordination environment of the metal ion, e.g. deprotonation of the coordinating water, resulting in the partial formation of $[RuA]^+$ (= $[RuAH(OH)]^+$). This is plausible for the γ-abhaH system as the pK_{RuAH} is rather high here compared to the other two ligands. Due to the fast exchange processes on the NMR time scale, the resonances of these two species appear as an averaged signal in the spectrum. The additional two sets of new doublets at pH = 6.23 may belong to two *p*-cym units being in different chemical environments in $[Ru_2AH_{-1}]^{2+}$. Above pH ~ 7 the spectra become rather complex. It is clear, however, that significant hydrolysis of the metal ion resulting in the formation of $[\{Ru(\eta^6\text{-}p\text{-cym})\}_2(\mu^2\text{-}OH)_3]^+$ (5.18 and 5.38 ppm)[20] does not occur up to pH = 11 in agreement with the speciation (Fig. 3c). Homonuclear 2D NMR experiments were also performed to gain additional information from the complex formation above pH ~ 7. While in the aromatic region of ^{1}H-^{1}H COSY spectrum (Fig. 7, red contour plot) cross-peaks can only be seen between ortho protons, in the same part of ^{1}H-^{1}H TOCSY spectrum (Fig. 7, black contour

plot) with long mixing time (120 ms) cross-peaks can also be seen between protons in meta and para position to each other. The careful evaluation of the TOCSY spectrum together with the COSY spectrum on the sample of pH = 8.52 (Fig. 7) has revealed that three main, individual $[(\eta^6\text{-}p\text{-cym})Ru]^{2+}$-containing spin systems existed in which all the *p*-cymene ring hydrogens became magnetically non-equivalent. This strongly suggests that both $[RuA]^+$ and $[RuAH_{-1}]_x$ (x = 1–2) in the form of binding isomers or dimers, as it is proposed in Fig. 4, may be present.

In order to model the interaction with DNA the binding capability of **2** with 9-methylguanine in aqueous solution was studied. As a representative example time dependence of the ^{1}H NMR spectra obtained is presented in Fig. 8. Since compound **2** does not have any resonances above 6 ppm, all signals shown in Figure 8 must be due to different guanine adducts (represented by the H8 resonances of 9-methylguanine). For the free ligand the H8 resonance is observed at 7.74 ppm (not shown here) at pH 7.0 in accordance with previous results.[51] At this resonance in Fig. 8 a broad signal of the free ligand is present (probably due to paramagnetic impurities in the NMR solvent). The other major resonances in the range 7.60–8.50 ppm clearly support that the guanine derivative interacts with **2**. The number of new signals indicate that, as a result of the binding of 9-methylguanine to the half-sandwich type metal core, diastereomers can be formed. Furthermore, the dissociation of the dinuclear metal complex and the formation of various adducts with the ligand can not be ruled out either. The binding is also supported by literature data where downfield shift of the H8 resonances was found for $[Ru(\eta^6\text{-bip})(en)]^{2+}$ (bip = biphenyl, en = ethylenediamine) containing an (N,N) chelator[56] while a slight upfield shift was detected for $[Ru(\eta^6\text{-}p\text{-cym})(acac)Cl]$ (acac = acetylacetonate) containing an (O,O) chelating set[57] upon reacting with 9-ethylguanine. Regarding the rate of the interaction the spectra suggest that this is fast (in accordance with earlier findings[56,57]) as no significant change in the ratio of the major signals in the function of time can be seen, however, two additional minor species also seem to be formed at a much slower rate.

3.4 Solid state structures

To obtain further proof for the existence and binding mode of the dinuclear complex suggested by pH-potentiometry and detected by ESI MS, solid state studies were also carried out. Treatment of the aqueous solutions containing the metal ion and α-alahaH with bromide or BF_4^- anions afforded dinuclear complexes as red crystalline solids in modest yield. The

compounds were characterized by elemental analysis, NMR, IR and ESI-MS methods (see 2.4 part for details). NMR showed the expected resonances of the methine and methyl protons of the ligand. IR spectra of the novel aminohydroxamate complexes exhibited a new sharp band at 1578 cm^{-1} compared to those of $[(\eta^6\text{-}p\text{-cym})RuCl_2]_2$ precursor which was assigned to the ν_{CO} of the coordinating hydroxamates. The BF_4^- anion in **2** was indicated by the chatacteristic streching at 1060 cm^{-1}.

Single crystal X-ray diffraction studies also revealed that **1** and **2** are indeed dinuclear ruthenium complexes in the solid state, too (Figs. 9 and 10). The structures of **1** and **2** are highly similar ones (Fig. S1) with some difference at the *p*-cym moiety only. Regarding other platium group metals search in the Cambridge Structural Database (Ver. 5.36 Update May, 2015.)[58] revealed no similar binding mode with bridging hydroxamate ligand among Ru, Rh, Ir, Os, Pd complexes. Only the platinum complex of pyridine-2-hydroxamate in κ^2-pyridine-2-hydroximato-N,N',O,O')-bis(cis-diammine-platinum(II)) had analogous [N,N][O,O] coordination geometry[59] but due to the pyridine moiety the structures are less comparable. Although this coordination fashion is quite abundant among copper and nickel hydroxamato compounds they are multinuclear rather than dinuclear complexes. In **1** and **2** the Ru–N and Ru–O distances for the hydroxamato ligands are in the expected range of 2.04–2.15 Å. The distance of the oxygen atom of the coordinated water molecule to the ruthenium center (Ru(1)–O(1)) is 2.204(5) Å and 2.191(5) Å for complex **1** and **2**, respectively. Due to steric requirements of the bulky *p*-cym ligand the angle of the mean planes of C-C-N-N-Ru and C-N-O-O-Ru is 17° for **1** and 16° for **2**. These are quite high values considering all the similarly [N,N][O,O] coordinated bridging hydroxamato complexes. Search of the CSD gave 106 hits for 2-aminohydroxamato or pyridine-2-hydroxamato complexes with [N,N] and [O,O] coordination in multinuclear metal complexes but only 25 hits remained when the angle of the coordination planes was limited into the range of 14° – 25°. These hits are pentameric copper, nickel or zinc hydroximato metallacrown complexes in which the cavity is occupied by a lanthanide ion resulting in similarly high steric constrains on the C-C-N-N and C-N-O-O planes of the bridging hydroximate-derivative ligand. Further bond distance and bond angle data can be found in the caption of Figs. 9 and 10. As alahaH in this study was racemic and two new stereogenic centers were formed on the Ru atoms upon coordination of the ligands we have a diastereomeric pair in the lattice forming a centrosymmetric space group. In this case the relative configuration of the stereogenic centers can be determined. Similar chiral-at-metal complexes have paramount importance in homogeneous catalytic processes.[60] However, there is no IUPAC recommendation for the nomenclature of the chirality of metal-

arene sandwich or half-sandwich complexes. Using an analogy[61] to the Cahn-Ingold-Prelog nomenclature suggests to use the pseudoatom convention by replacing the *p*-cym ligand with a pseudoatom with an atomic weight of 6 x 12 = 72 amu. Although the complexes **1** and **2** are homochiral ones (Fig. S1) this convention results in change in the priority rules causing opposite assignment for Ru(2). Hence the relative configuration of complex **1** is $S^*_{C(1)},R^*_{Ru(1)},R^*_{Ru(2)}$ while that of complex **2** is $S^*_{C(1)},R^*_{Ru(1)},S^*_{Ru(2)}$.

Cytotoxicity in cancer cells

The *in vitro* anti-cancer chemotherapeutic potential of complexes **1** and **2** towards a set of various human cancer cell lines (A2780, MCF-7, HeLa, SKOV-3 and HCT-116) was also tested. To determine cytotoxic effect of the compounds NR assay have been employed. This assay is based on the ability of viable cells to incorporate and bind the dye in lysosomes by an active metabolic process. The results clearly showed that the complexes tested in this work caused very low or insignificant cytotoxic effect (Fig. 11) even in the highest concentration tested in this work (0.5 mM). In contrast, cisplatin displayed a significant reduction in viability of the cells under the same conditions with the mean IC_{50} values of 1.8 ± 0.2 μM, 8.2 ± 1.0 μM, 1.9 ± 0.1 μM, 12.1± 2.1 μM and 7.4 ± 0.7 μM for A2780, MCF-7, HeLa, Skov-3, and HCT-116 cells, respectively. Thus, compounds **1** and **2** expressed cytotoxic activity more than two order of magnitude lower than cisplatin, even in those cancer cells inherently resistant to cisplatin.

4. Conclusions

Previously simple hydroxamates were proven to be effective binders for half-sandwich type Ru(II) at pH = 7.4[18], but high thermodynamic stability of the complexes was accompanied by labile kinetic behaviour. These fast ligand exchange processes seemed to count for ineffective anticancer activity found on human-derived A2780 and A2780R cell lines.

Our results in this study indicate that the presence of an amino group in chelatable position to the primary hydroxamate function in aminohydroxamates provides effective ligands for binding a half-sandwich type Ru(II). These molecules were shown to be capable of preventing the metal ion from hydrolysis up to pH ~ 11 and can also bind a second metal ion. Partially slow complex formation processes under weakly acidic conditions for the α and β but not for the γ derivative seem to be correlated with the size of the (N,N) chelate that can

also be found with these ligands beside the (O,O) hydroxamate one. This more inert kinetic behaviour made especially α-alaha a promising candidate for biological tests. Moreover, **2** was shown to react with 9-methylguanine (as a DNA model) in a fast reaction. However, the results of the cell line studies indicated that **1** and **2** both sharing very similar binding architecture are not effective in the micromolar concentration range against the A2780, MCF-7, HeLa, Skov-3, and HCT-116 cell lines.

Acknowledgments

The authors thank members of the EU COST Action CM1105 for motivating discussions. This work was supported by the Hungarian Scientific Research Fund (OTKA K112317 and NK105691). The research of J.K. and T.R-M. was also supported by the Ministry of Education, Youth and Sports of the CR (Grant LH 14317) and by Palacky University in Olomouc (IGAPrF2015025).

References

[1] A.M. Albrecht-Gary, A.L. Crumbliss, *Metal Ions in Biological Systems* **1998**, *35*, 239-327.
[2] H. Boukhalfa, A.L. Crumbliss, *Biometals* **2002**, *15*, 325-339.
[3] C.J. Marmion, J.P. Parker, K.B. Nolan, Hydroxamic Acids: An Important Class of Metalloenzyme Inhibitors. In: Jan Reedijk and Kenneth Poeppelmeier, Eds, Elsevier, Comprehensive Inorganic Chemistry II: From Elements to Applications, **2013**, *3*, 684-708.
[4] E.M.F. Muri, M.J. Nieto, R.D. Sindelar, J.S. Williamson, *Curr. Med. Chem*. **2002**, *9*, 1631-1653.
[5] P.A. Marks, *Oncogene* **2007**, *26*, 1351–1356.
[6] M. Melchart, P.J. Sadler, in *Bioorganometallics*, ed. G. Jaouen, Wiley-VCH, Weinheim, Germany, **2006**, p. 39-64.
[7] B. Therrien, *Coord. Chem. Rev*. **2009**, *253*, 493–519.
[8] P.C.A. Bruijnincx, P.J. Sadler, *Adv. Inorg. Chem.* **2009**, *61*, 1-62.
[9] G. Süss-Fink, *Dalton Trans.* **2010**, *39*, 1673-1688.
[10] I. Bratsos, T. Gianferrara, E. Alessio, C.G. Hartinger, M.A. Jakupec, B.K. Keppler, in *Bioinorganic Medicinal Chemistry*, ed. E. Alessio, Wiley-VCH, Weinheim, Germany, **2011**, p. 160-164.
[11] H. Chen, J.A. Parkinson, R.E. Morris, P.J. Sadler, *J. Am. Chem. Soc*. **2003**, *125*, 173-186.
[12] O. Novakova, H. Chen, O. Vrana, A. Rodger, P. J. Sadler, V. Brabec, *Biochemistry*, **2003**, *42*, 11544-11-554.
[13] H-K. Liu, S.J. Berners-Price, F. Wang, J.A. Parkinson, J. Xu, J. Bella, P.J. Sadler, *Angew. Chem. Int. Ed. Engl*. **2006**, *45*, 8153-8156.
[14] A.M. Pizarro, P.J. Sadler, *Biochimie*, **2009**, *91*, 1198-1211, and references therein.
[15] V. Moreno, M. Font-Bardia, T. Calvet, J. Lorenzo, F.X. Avilés, M.H. Garcia, T.S. Morais, A. Valente, M.P. Robalo, *J. Inorg. Biochem*., **2011**, *105*, 241-249.

[16] A.I. Tomaz, T. Jakusch, T.S. Morais, F. Marques, R.F.M. de Almeida, F. Mendes, É.A. Enyedy, I. Santos, J. Costa Pessoa, T. Kiss, M.H. Garcia, *J. Inorg. Biochem*., **2012**, *117*, 261-269.

[17] T.S. Morais, F. Santos, L. Côrte-Real, F. Marques, M.P. Robalo, P.J.A. Madeira, M.H. Garcia, *J. Inorg. Biochem*. **2013**, *122*, 8-17.

[18] P. Buglyó, E. Farkas, *Dalton Trans*. **2009**, 8063-8070.

[19] L. Bíró, E. Farkas, P. Buglyó, *Dalton Trans*. **2010**, *39*, 10272-10278.

[20] L. Bíró, E. Farkas, P. Buglyó, *Dalton Trans*. **2012**, *41*, 285-291.

[21] L. Bíró, D. Hüse, A.C. Bényei, P. Buglyó, *J. Inorg. Biochem*. 2012, *116*, 116-125.

[22] É.A. Enyedy, G.M. Bognár, T. Kiss, M. Hanif, C.G. Hartinger, *J. Organomet. Chem*. **2013**, *734*, 38-44.

[23] L. Bíró, E. Balogh, P. Buglyó, *J. Organomet. Chem*. **2013**, *734*, 61-68.

[24] A. Kurzwernhart, W. Kandioller, É.A. Enyedy, M.Novak, M.A. Jakupec, B.K. Keppler, C.G. Hartinger, *Dalton Trans*. **2013**, *42*, 6193-6202.

[25] É.A. Enyedy, É. Sija, T. Jakusch, C.G. Hartinger, W. Kandioller, B.K. Keppler, T. Kiss, *J. Inorg. Biochem*. **2013**, *127*, 161-168.

[26] D. Hüse, L. Bíró, J. Patalenszki, A.C. Bényei, P. Buglyó, *Eur. J. Inorg. Chem*. **2014**, 5204-5216.

[27] É. Sija, C.G. Hartinger, B.K. Keppler, T. Kiss, É.A. Enyedy, *Polyhedron* **2014**, *67*, 51-58.

[28] Zs. Bihari, Z. Nagy, P. Buglyó, *J. Organomet. Chem*. **2015**, *782*, 82-88.

[29] J. Patalenszki, L. Bíró, A.C. Bényei, T.R. Muchova, J. Kasparkova, P. Buglyó, *RSC Adv.* **2015**, *5*, 8094-8107.

[30] A.J. Godó, A.C. Bényei, B. Duff, D.A. Egan, P. Buglyó, *RSC Adv*. **2012**, *2*, 1486–1495.

[31] A.F.A. Peacock, A. Habtemariam, R. Fernandez, V. Walland, F.P.A. Fabbiani, S. Parsons, R.E. Aird, D.I. Jodrell, P.J. Sadler, *J. Am. Chem. Soc*. **2006**, *128*, 1739-1748.

[32] B. Kurzak, H. Kozlowski, E. Farkas, *Coord, Chem. Rev*. **1992**, *114*, 169-200.

[33] B. Kurzak, E. Farkas, *J. Coord. Chem*. **1993**, 28, 203-207.

[34] E. Farkas, K. Megyeri, L. Somsák, L. Kovács, *J. Inorg. Biochem*. **1998**, 70, 41-47.

[35] E. Farkas, H. Csóka, G. Bell, D.A. Brown, L.P. Cuffe, N.J. Fitzpatrick, W.K. Glass, W. Errington, T.J. Kemp, *J. Chem. Soc., Dalton Trans*. **1999**, 2789-2794.

[36] P. O`Sullivan, J.D. Glennon, E. Farkas, T. Kiss, *J. Coord. Chem*. **1996**, 38, 271-280.

[37] É.A. Enyedy, H. Csóka, I. Lázár, G. Micera, E. Garribba, E. Farkas, *J. Chem. Soc., Dalton Trans*. **2002**, 2632-2640.

[38] B. Kurzak, E. Farkas, T. Glowiak, H. Kozlowski, *J. Chem. Soc., Dalton Trans*. **1991**, 163-167.

[39] V.L. Pecoraro, A.J. Stemmler, B.R. Gibney, J.J. Bodwin, H. Wang, J.W. Kampf, A. Barwinski in *Metallacrowns: A New Class of Molecular Recogntition Agents*, Progress in Inorganic Chemistry, ed.: K. D. Karlin, John Wiley, New York, **1997**, vol. 45.

[40] D.D. Perrin, W.L.F. Armarego, Purification of Laboratory Chemicals, 3rd ed., Pergamon, Oxford, **1988**.

[41] A.H. Blatt, *Organic Synthesis Collection* **1943**, Wiley, New York, Vol. 2, p. 67.

[42] M.A. Bennett, A.K. Smith, *J. Chem. Soc., Dalton Trans*. **1974**, 233–241.

[43] A. Altomare, G. Cascarano, C. Giacovazzo, A. Guagliardi, *J. Appl. Cryst*. **1993**, *26*, 343-350.

[44] G.M. Sheldrick, *Acta Cryst.* **2008**, *A64*, 112-122.

[45] L.J. Farrugia, *J. Appl. Cryst.* **1999**, *32*, 837-838.

[46] S.P. Westrip, *J. Appl. Cryst.*, **2010**, *43*, 920-925.

[47] G. Gran, *Acta Chem. Scand*., **1950**, *4*, 559–577.

[48] H.M. Irving, M.G. Miles, L.D. Pettit, *Anal. Chim. Acta*, **1967**, *38*, 475–488.

[49] L. Zékány and I. Nagypál, in: D. Leggett (Ed.), *Computational Methods for the Determination of Stability Constants*, Plenum, New York (1985).
[50] P. Gans, A. Sabatini, A. Vacca, *J. Chem Soc., Dalton Trans*. **1985**, 1195–1200.
[51] N. Busto, J. Valladolid, M. Martínez-Alonso, H.J. Lozano, F.A. Jalón, B.R. Manzano, A.M. Rodríguez, M.C. Carrión, T. Biver, J.M. Leal, G. Espino, B. García, *Inorg. Chem*., **2013**, *52*, 9962-9974.
[52] V. Novohradsky, L. Zerzankova, J. Stepankova, A. Kisova, H. Kostrhunova, Z. Liu, P.J. Sadler, J. Kasparkova, V. Brabec, *Metallomics*, **2014**, *6*, 1491-1501.
[53] E. Farkas, T. Kiss, B. Kurzak, *J. Chem. Soc., Perkin Trans*. **1990**, *2*, 1255-1257.
[54] D. Bátka, Ph.D. Thesis, University of Debrecen, **2007**.
[55] O. Szabó, Ph.D. Thesis, University of Debrecen, **2013**.
[56] H. Chen, J.A. Parkinson, S. Parsons, R.A. Coxall, R.O. Gould, P.J. Sadler, *J. Am. Chem. Soc.*, **2002**, *124*, 3064-3082.
[57] R. Fernández, M. Melchart, A. Habtemariam, S. Parsons, P.J. Sadler, *Chem. Eur. J.*, **2004**, *10*, 5173-5179.
[58] F.R. Allen, *Acta Crystallogr., Sect. B: Struct. Sci*., **2002**, *58*, 380-388.
[59] D. Griffith, K. Lyssenko, P. Jensen, P.E. Kruger, C.J. Marmion, Dalton Trans., **2005**, 956-961.
[60] *Chirality in Transition Metal Chemistry: Molecules, Supramolecular Assemblies and Materials*, Eds. H. Amouri and M. Gruselle, Wiley, **2008**, pp. 65-97.
[61] *Bioorganometallic Chemistry Applications in Drug Discovery, Biocatalysis, and Imaging*, Eds. G. Jaouen and M. Salmain, Wiley, **2015**, pp. 89-90.

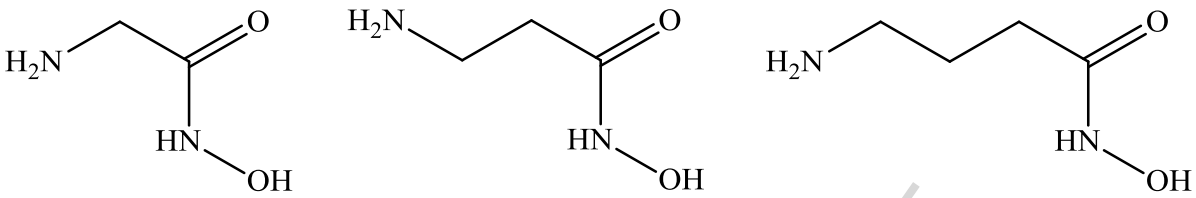

α-alahaH β-alahaH γ-abhaH

Figure 1. Structure of the neutral form and abbreviation of the ligands studied.

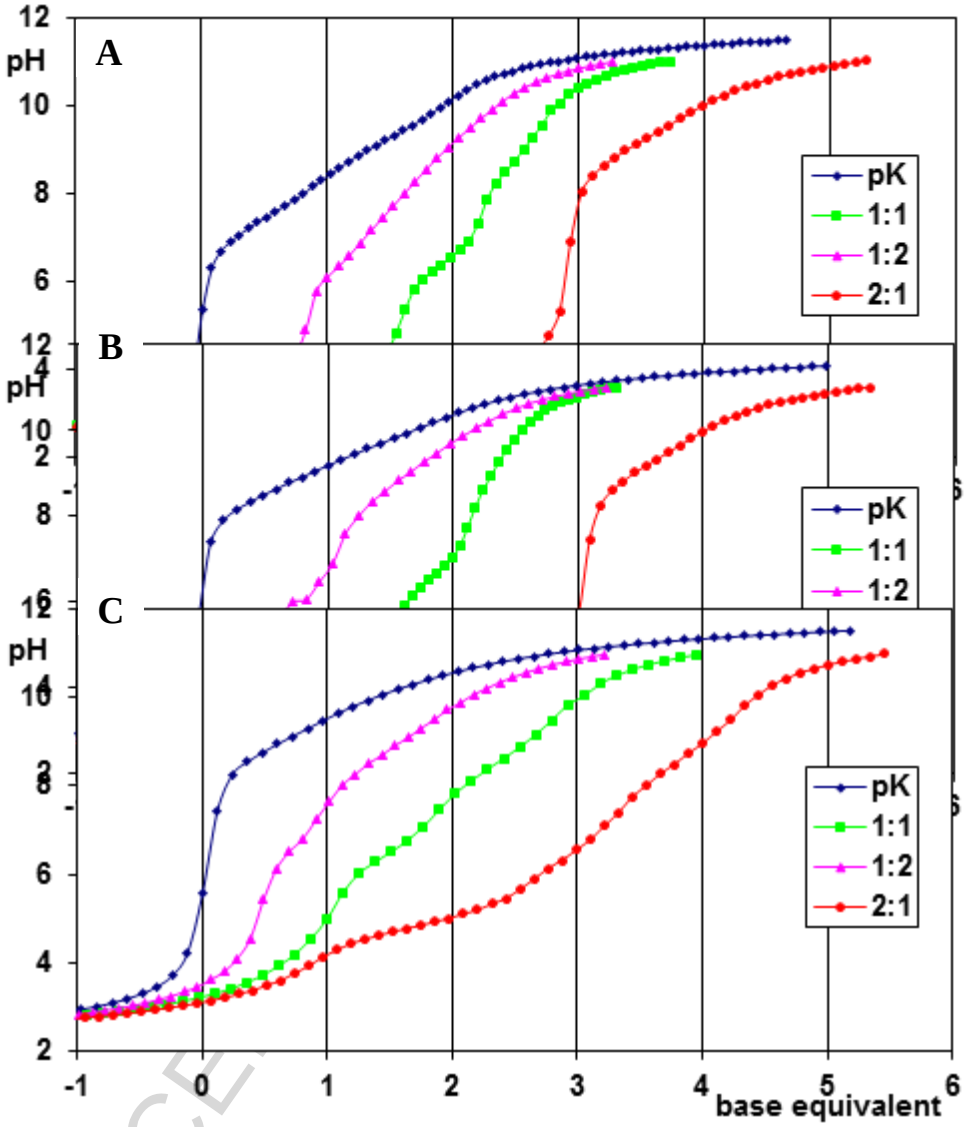

Figure 2. Titration curves for the H^+ – ligand (pK) and the $[(\eta^6\text{-}p\text{-cym})Ru(H_2O)_3]^{2+}$ – ligand systems at various (1:1, 1:2 and 2:1) ratios with α-alahaH (A), β-alahaH (B) and γ-abhaH (C). Negative base equivalent refers to an excess of acid in the sample.

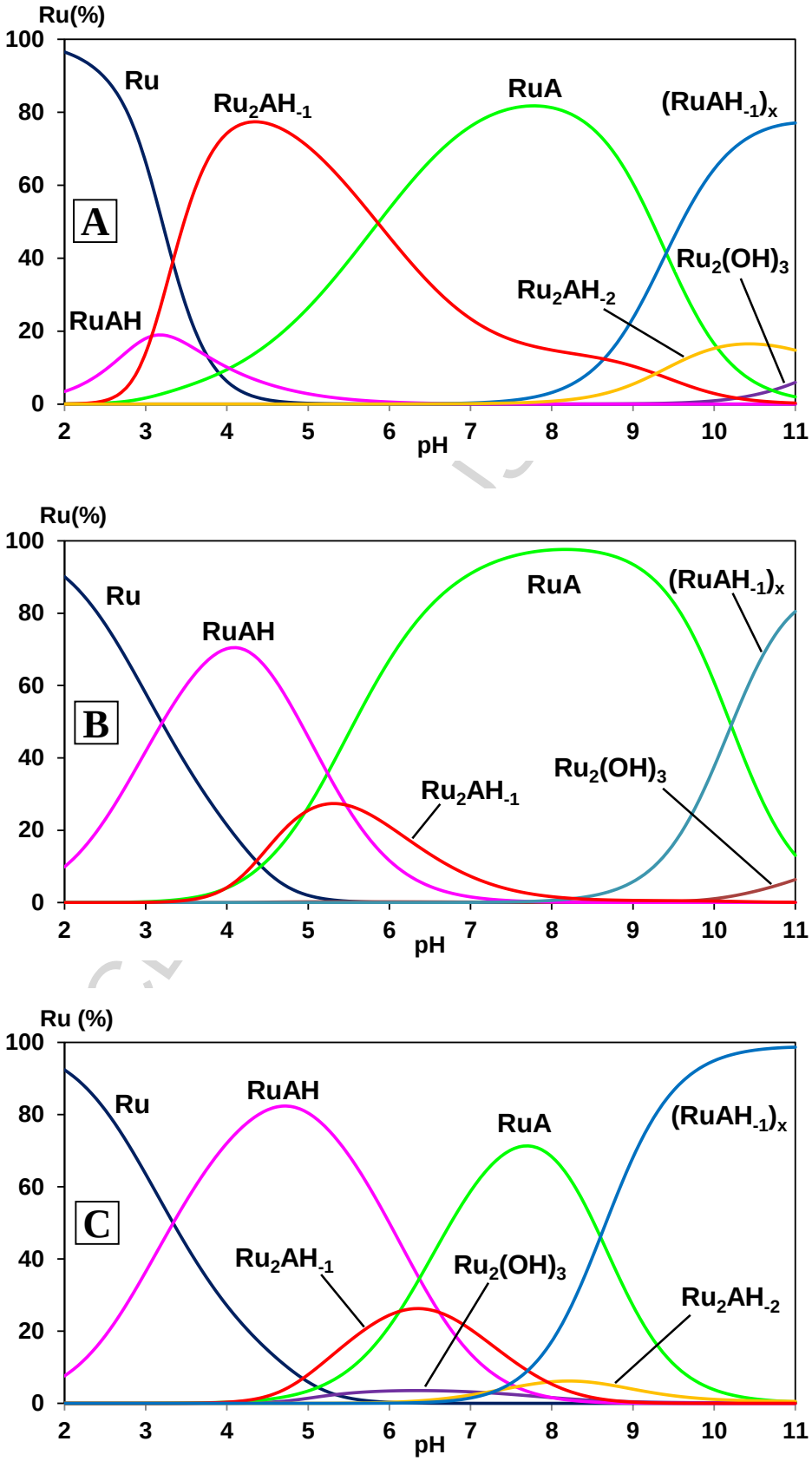

Figure 3. Calculated concentration distribution curves for the $[(\eta^6\text{-}p\text{-cym})Ru(H_2O)_3]^{2+}$–α-alaha (A), –β-alaha (B) and –γ-alaha (C) systems at 1:1 metal ion to ligand ratio. c_{Ru} = 4.0 mM. „Ru" refers to $[(\eta^6\text{-}p\text{-cym})Ru]^{2+}$.

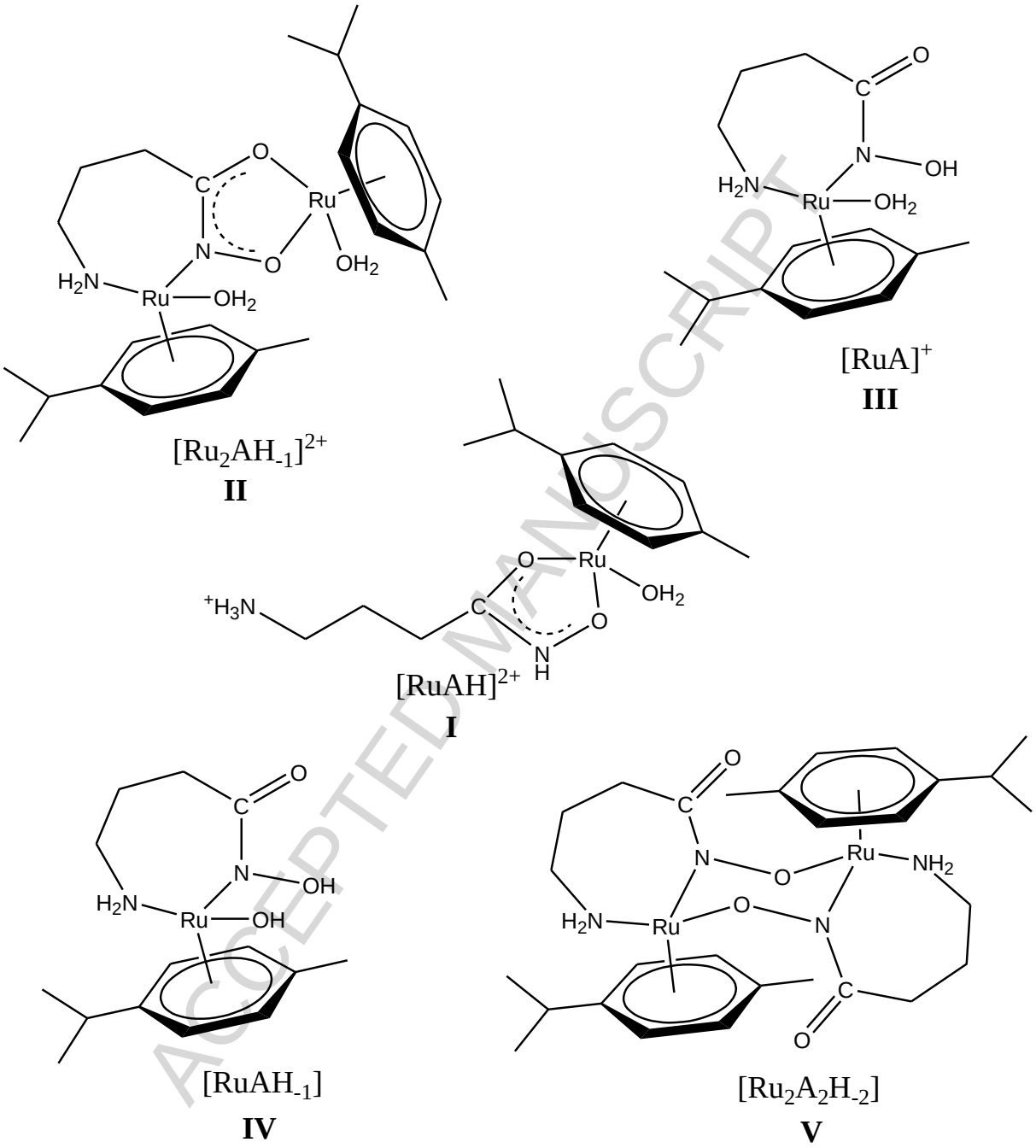

Figure 4. Plausible solution structures of the aminohydroxamate complexes (in this case with the γ-abha).

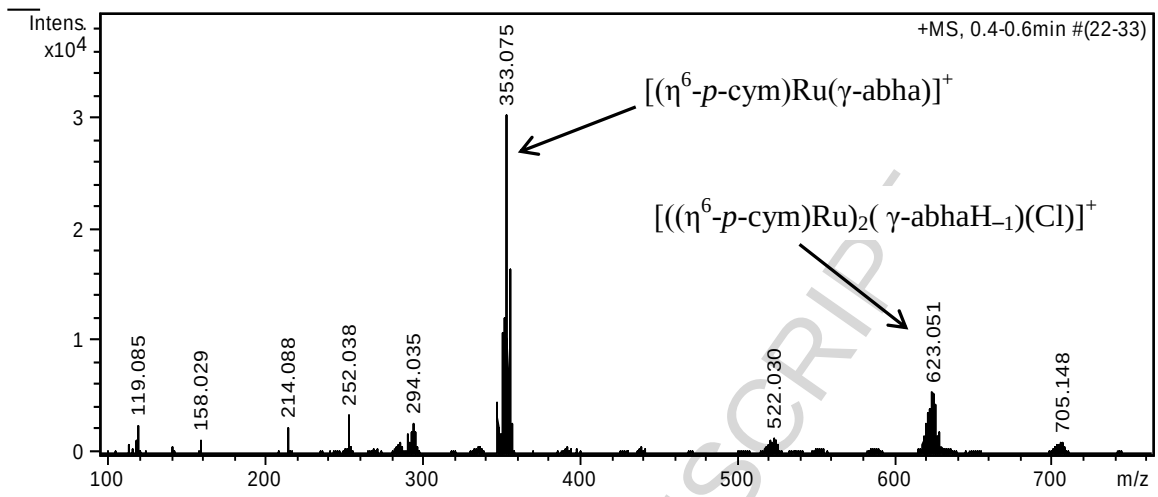

Figure 5. ESI-MS spectrum of the $[(\eta^6\text{-}p\text{-cym})Ru(H_2O)_3]^{2+}$ - γ-abha system at 1:1 metal ion to ligand ratio (pH = 6.07).

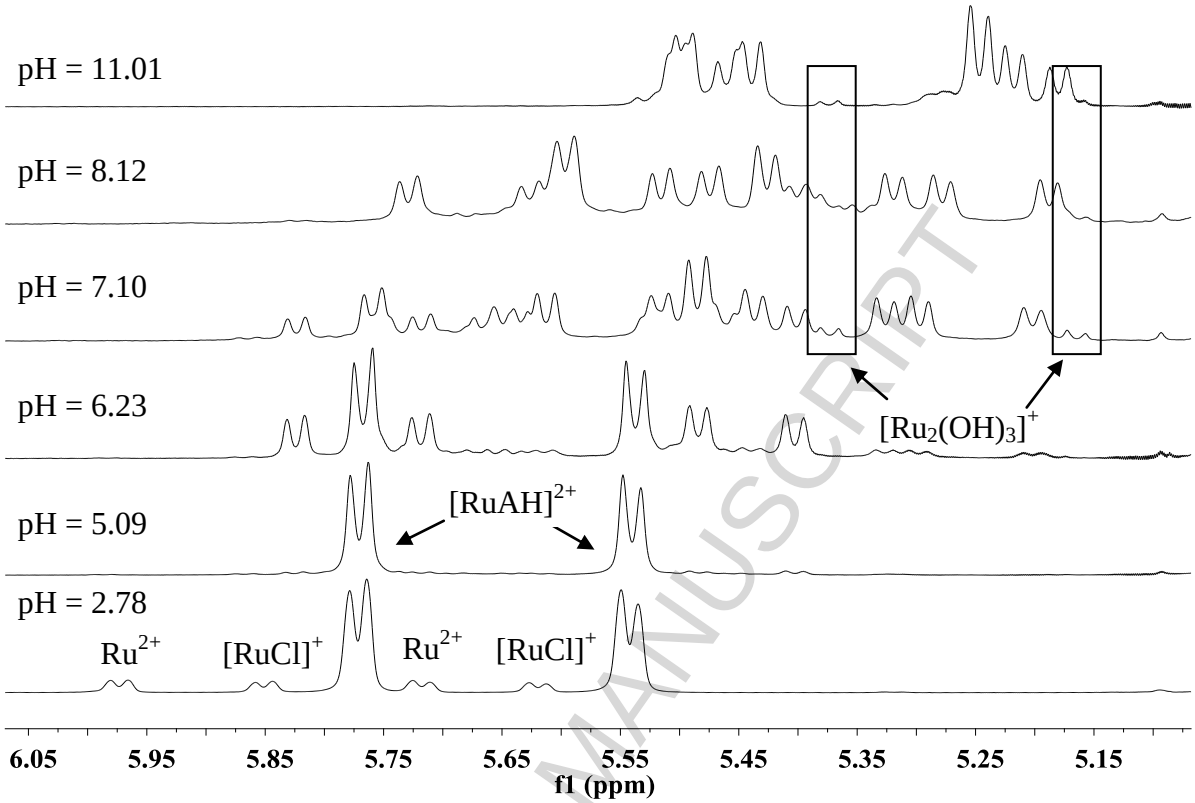

Figure 6. Dependence on pH of the aromatic region of the ^{1}H NMR spectra of [(η^6-*p*-cym)Ru(H_2O)$_3$]$^{2+}$–γ-abhaH system at 278 K in D_2O, 1:1 metal ion to ligand ratio, c_{Ru} = 10 mM). „Ru" stands for [(η^6-*p*-cym)Ru]$^{2+}$.

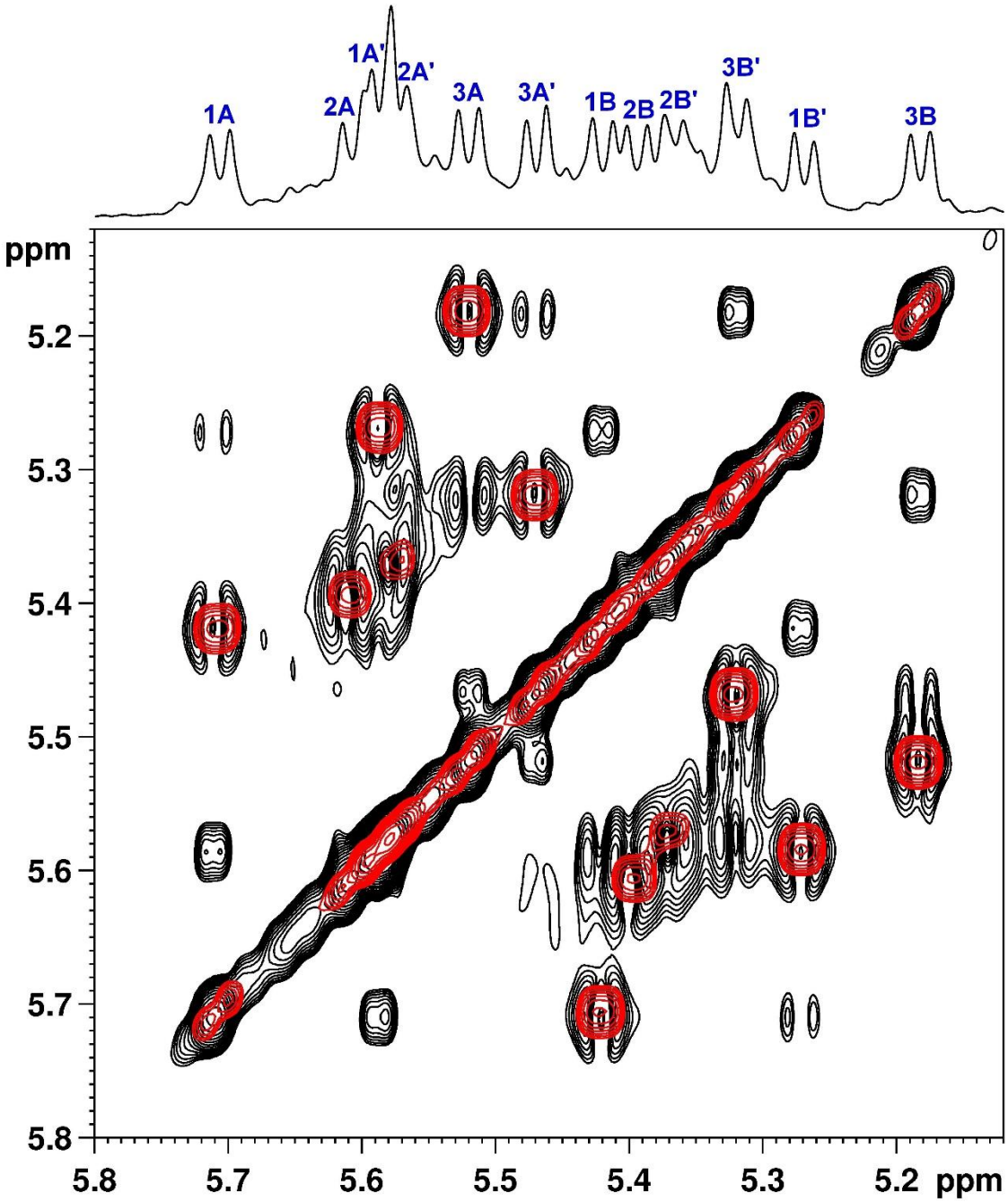

Figure 7. The aromatic region of ^{1}H-^{1}H COSY (red), TOCSY (black) and ^{1}H NMR spectrum (above the 2D contour plots) of the $[(\eta^{6}\text{-}p\text{-cym})Ru(H_2O)_3]^{2+}$ - γ-abhaH system, 1:1 metal ion to ligand ratio, pH = 8.52. Assignment is shown above the ^{1}H NMR spectrum and indicates three distinct spin systems (1A, 1A', 1B, 1B' / 2A, 2A', 2B, 2B' / 3A, 3A', 3B, 3B').

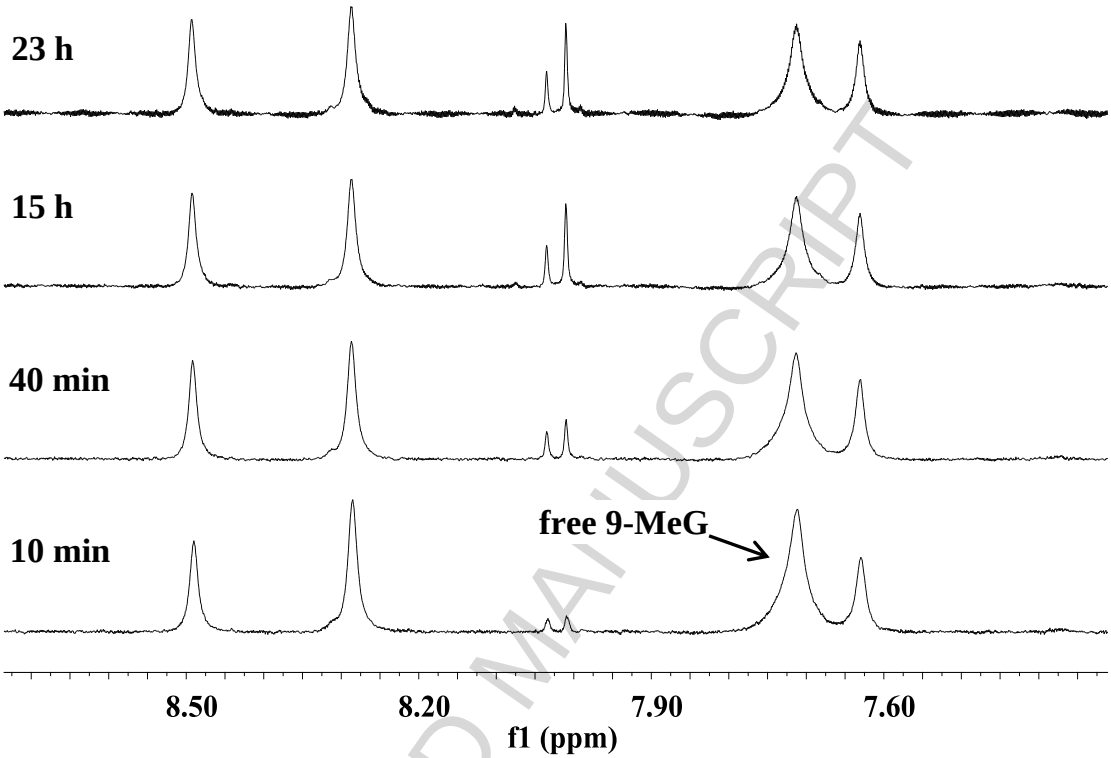

Figure 8. Low field region of the ^{1}H NMR spectra for the reaction between complex **2** and 9-methylguanine (9-MeG) (1:2 mol ratio; pH = 7) after 10 min, 40 min, 15 h and 23 h in D_2O. Concentration of **2** was 2 mM.

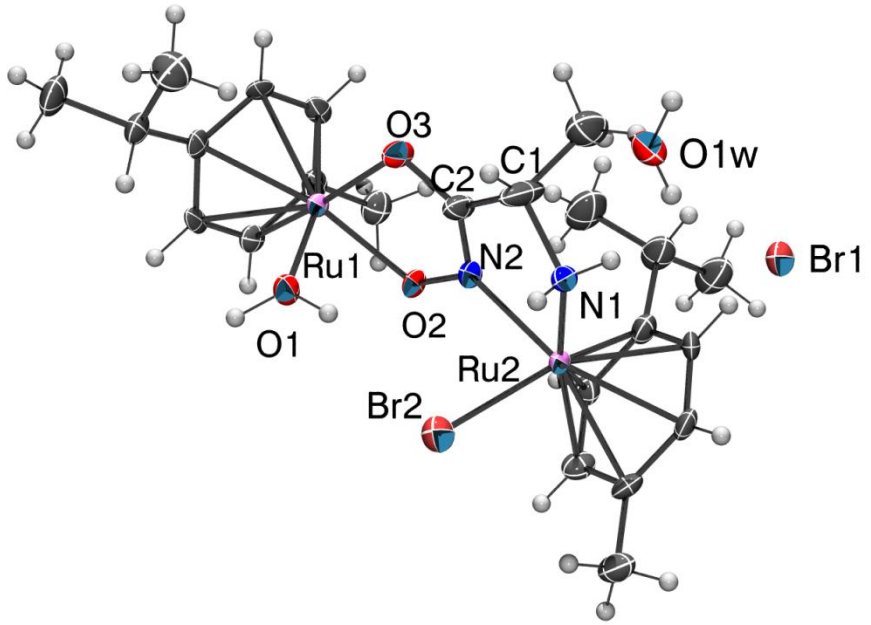

Figure 9. ORTEP view of [{(η^6-p-cym)Ru}$_2$(μ^2-α-alahaH$_{-1}$)(H_2O)Br]Br·H_2O (**1**) at 50% probability level. Selected bond lengths [Å] and angles [^{o}]: Br(2)–Ru(2) 2.5324(11), C(1)–N(1) 1.496(9), C(1)–C(2) 1.515(11), C(2)–O(3) 1.301(9), C(2)–N(2) 1.308(10), O(3)–Ru(1) 2.071(5), N(1)–Ru(2) 2.142(6), N(2)–O(2) 1.408(7), N(2)–Ru(2) 2.048(6), O(1)–Ru(1) 2.204(5), O(2)–Ru(1) 2.034(5), O2-Ru1-O3 79.6(2), O2-Ru1-O1 80.8(2), O3-Ru1-O1 81.3(2), N2-Ru2-Br2 83.53(18), N1-Ru2-Br2 83.24(18), N2-Ru2-N1 77.0(2).

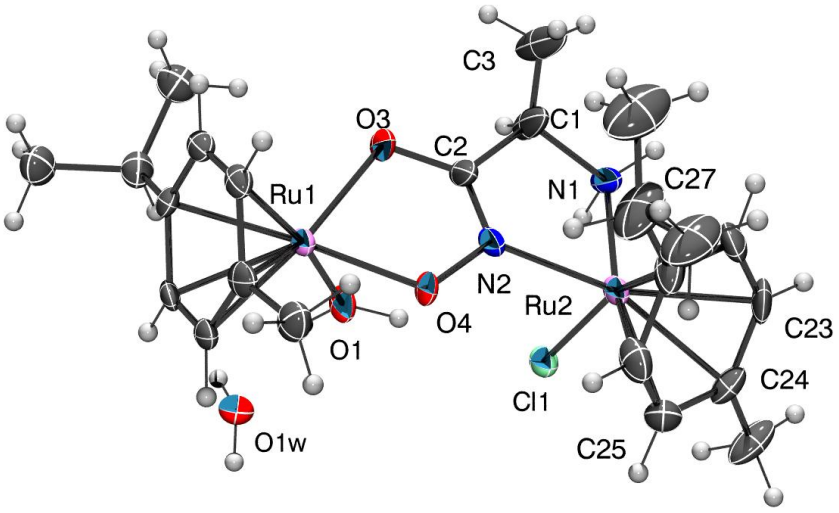

Figure 10. ORTEP view of [{(η^6-*p*-cym)Ru}$_2$(μ^2-α-alahaH$_{-1}$)(H_2O)Cl]BF_4·H_2O (**2**) at 40% probability level, BF_4^- counter ion was omitted for clarity. For the disordered i-Pr moiety of the cymene ligand only the major isomer is shown. Selected bond lengths [Å] and angles [^{o}]: C(1)–C(3) 1.257(17), Cl(1)–Ru(2) 2.431(2), C(1)–N(1) 1.483(11), N(1)–Ru(2) 2.147(8), C(1)–C(2) 1.528(13), N(2)–O(4) 1.402(8), C(2)–N(2) 1.296(13), N(2)–Ru(2) 2.048(6), C(2)–O(3) 1.304(10), O(1)–Ru(1) 2.191(5), O(3)–Ru(1) 2.075(5), O(4)–Ru(1) 2.042(5), O4-Ru1-O3 79.7(2), O4-Ru1-O1 80.6(2), O3-Ru1-O1 80.0(3), N2-Ru2-N1 76.3(3), N2-Ru2-Cl1 83.3(2), N1-Ru2-Cl1 83.2(3).

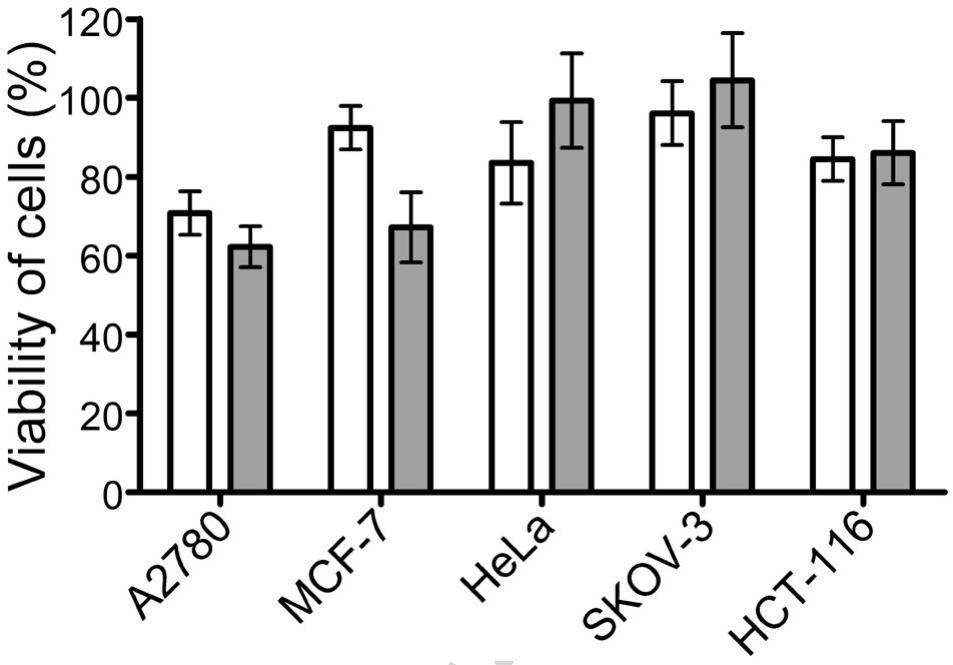

Figure 11. Bar graph representation of cell viability data as determined by NR assay performed with indicated cell lines following their exposure to 0.5 mM concentrations of compounds **1** (open bars) and **2** (full bars). Values are represented in percentage with control (untreated cells) taken as 100%. The error bars represent the standard deviation of the mean (± SD).

Table 1. Crystallographic data and structure refinement results for [{(η^6-*p*-cym)Ru}$_2$(μ^2-α-alahaH$_{-1}$)(H_2O)Br]Br·H_2O (**1**) and [{(η^6-*p*-cym)Ru}$_2$(μ^2-α-alahaH$_{-1}$)(H_2O)Cl]BF_4·H_2O (**2**).

Compound	**1**	**2**
Formula	$C_{23}H_{38}Br_2N_2O_4Ru_2$	$C_{23}H_{38}ClN_2O_4Ru_2BF_4$
Formula weight	768.51	730.95
Crystal system	Triclinic	Triclinic
Space group (No.)	P-1 (2)	P-1 (2)
a / Å	9.6941(6)	10.2430(7)
b / Å	10.4848(7)	10.3294(9)
c / Å	14.2904(9)	14.3419(13)
α / °	72.046(6)	75.204(8)
β / °	75.966(6)	72.031(7)
γ / °	76.755(6)	77.540(7)
V / Å^3	1321.63(16)	1380.0(2)
Z	2	2
D_c / g cm^{-3}	1.931	1.759
F(000)	760	736
μ / mm^{-1}	13.05	10.28
Reflections collected	9843	10506
Unique reflections	5085	5308
Reflections with I > 2σ(I)	4278	4163
Parameters refined	323	409
GOF[a] on F^2	1.04	1.02
R[b] [$F^2 > 2\sigma(F^2)$]	0.057	0.063
R_{int}	0.045	0.058
$wR(F^2)$[b]	0.164	0.170
$\Delta\rho_{max}$, $\Delta\rho_{min}$ / e Å^{-3}	2.69, -2.22	1.66, -0.89

[a] GOF = $[\Sigma\omega(F_o^2 - F_o^2)^2/(n-p)]^{1/2}$

[b] $R_1 = \Sigma \big| |F_o| - |F_c| \big| / \Sigma |F_o|$, $\omega R_2 = [\Sigma\omega(F_o^2 - F_o^2)^2/\Sigma\omega F_o^2]^{1/2}$

Table 2. Stepwise protonation constants (log*K*) of the aminohydroxamates and stability constants (log*β*) of their $[(\eta^6\text{-}p\text{-cym})Ru]^{2+}$ complexes at 25.0 °C and I = 0.20 M KCl.†

species	α-alahaH		β-alahaH		γ-abhaH	
HA	9.18 (1)		9.75 (1)		10.19 (1)	
H_2A^+	7.36 (1)		8.48 (1)		8.77 (1)	
	model A	model B	model A	model B	model A	model B
$[RuAH]^{2+}$	*15.86(7)*	*15.85(7)*	*17.99(3)*	*17.99(3)*	18.71(1)	18.71(1)
$[RuA]^+$	*11.83(10)*	*11.78(10)*	*12.75(8)*	*12.74(9)*	12.34(4)	12.34(4)
$[RuAH_{-1}]$	*2.42(8)*	–	*2.54(10)*	–	3.74(4)	–
$[Ru_2A_2H_{-2}]$	–	*7.7(2)*	–	*7.9(2)*	–	10.51(8)
$[Ru_2AH_{-1}]^{2+}$	*12.38(3)*	*12.38(3)*	*11.83(7)*	*11.82(7)*	11.45(5)	11.46(5)
$[Ru_2AH_{-2}]^+$	*3.1(1)*	*3.31(10)*	–	–	3.50(12)	3.92(8)
pK_{RuAH}	*4.03*	*4.07*	*5.24*	*5.25*	6.37	
pK_{RuA}	*9.41*	–	*10.21*	–	8.60	–
$\log K^*_{RuAH}$ [a]	–0.68		–0.24		–0.25	
$\log K^*_{RuA}$ [b]	–4.73		–5.48		–6.62	
fitting parameter[#] (ml)	0.0154	0.0163	0.0173	0.0188	0.0058	0.0063
number of data points	203		245		215	

† 3σ standard deviations are in parantheses; „Ru" stands for the $[(\eta^6\text{-}p\text{-cym})Ru]^{2+}$ entity.

[#] Fitting parameter is the average difference between the calculated and experimental titration curves expressed in mL of the titrant.

[a] Refers to the following proton displacement equilibrium: $Ru^{2+} + H_2A^+ = [RuAH]^{2+} + H^+$.

[b] Refers to the following proton displacement equilibrium: $Ru^{2+} + H_2A^+ = [RuA]^+ + 2H^+$.

Table 3. Observed species with their calculated m/z values in the $[(\eta^6\text{-}p\text{-cym})Ru(H_2O)_3]^{2+}$–aminohydroxamic acid 1:1 systems using ESI-TOF-MS.[#]

Species	m/z (observed)	m/z (calculated)
$[(\eta^6\text{-}p\text{-cym})RuCl]^+$	270.980	270.982
$[(\eta^6\text{-}p\text{-cym})Ru(\alpha\text{-alaha})]^+$	339.069[a]	339.064
$[((\eta^6\text{-}p\text{-cym})Ru)_2(\alpha\text{-alahaH}_{-1})]^{2+}$	286.535	286.536
$[(\eta^6\text{-}p\text{-cym})Ru(\alpha\text{-alaha})]^+$	339.069[b]	339.064
$[((\eta^6\text{-}p\text{-cym})Ru)_2(\alpha\text{-alahaH}_{-1})_2] + H^+$	677.150	677.123
$[((\eta^6\text{-}p\text{-cym})Ru)_2(\alpha\text{-alahaH}_{-1})_2] + K^+$	715.109	715.078
$[(\eta^6\text{-}p\text{-cym})Ru(\beta\text{-alaha})]^+$	339.059	339.064
$[(\eta^6\text{-}p\text{-cym})Ru(\beta\text{-alahaH}_{-1})] + K^+$	377.014	377.020
$[((\eta^6\text{-}p\text{-cym})Ru)_2(\beta\text{-alahaH}_{-1})_2] + H^+$	677.117	677.123
$[((\eta^6\text{-}p\text{-cym})Ru)_2(\beta\text{-alahaH}_{-1})_2] + K^+$	715.071	715.078
$[(\eta^6\text{-}p\text{-cym})Ru(\gamma\text{-abha})]^+$	353.075	353.080
$[((\eta^6\text{-}p\text{-cym})Ru)_2(\gamma\text{-abhaH}_{-1})(Cl)]^+$	623.051	623.056
$[((\eta^6\text{-}p\text{-cym})Ru)_2(\gamma\text{-abhaH}_{-1})_2] + H^+$	705.149	705.154
$[((\eta^6\text{-}p\text{-cym})Ru)_2(\gamma\text{-abhaH}_{-1})_2] + K^+$	743.104	743.110

[#]„ α-alaha", „β-alaha" and „γ-abha" stand for the fully deprotonated ligands. [a] measured at pH = 2.56. [b] measured at pH = 9.50

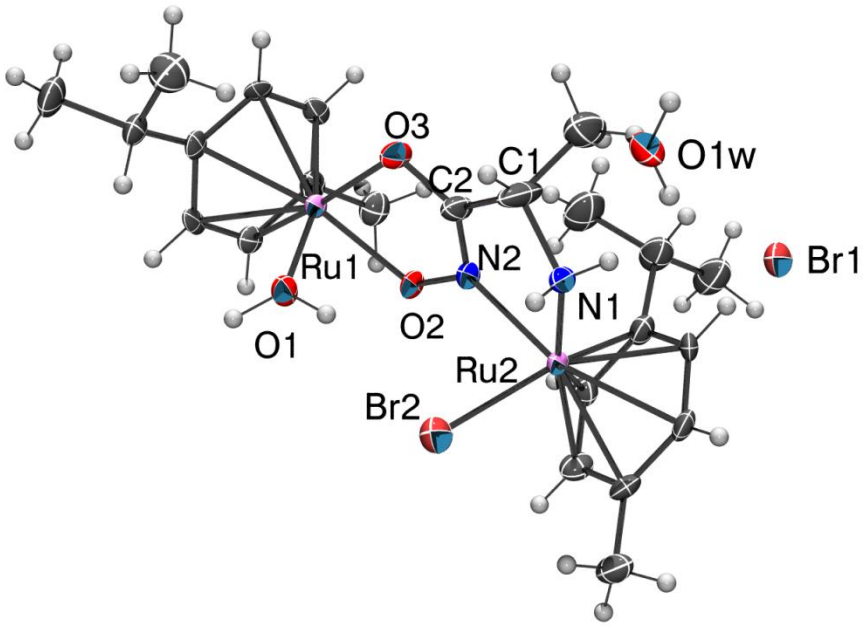

Graphical abstract

Graphical abstract synopsis

The interaction between $[Ru(\eta^6\text{-}p\text{-cymene})(H_2O)_3]^{2+}$ and various aminohydroxamates was studied with the aid of combined pH-potentiometric, ^{1}H-NMR and ESI-TOF-MS methods in aqueous solution, furthermore, the crystal and molecular structure of $[\{Ru(\eta^6\text{-}p\text{-cymene})\}_2(\mu^2\text{-}\alpha\text{-alahaH}_{-1})(H_2O)Br]Br\cdot H_2O$ and $[\{Ru(\eta^6\text{-}p\text{-cymene})\}_2(\mu^2\text{-}\alpha\text{-alahaH}_{-1})(H_2O)Cl]BF_4\cdot H_2O$ (α-alaha = 2-amino-N-hydroxyacetamide) was determined by X-ray diffraction method.

Highlights

- Solution study of $[Ru(\eta^6\text{-}p\text{-cymene})(H_2O)_3]^{2+}$–α-, β- and γ-aminohydroxamate (alaha) systems
- Demonstration of the formation of highly stable, partly dinuclear complexes
- Lack of hydrolysis of the metal ion under biologically relevant conditions
- X-ray characterization of $[\{Ru(\eta^6\text{-}p\text{-cymene})\}_2(\mu^2\text{-}\alpha\text{-alahaH}_{-1})(H_2O)Br]Br\cdot H_2O$
- X-ray characterization of $[\{Ru(\eta^6\text{-}p\text{-cymene})\}_2(\mu^2\text{-}\alpha\text{-alahaH}_{-1})(H_2O)Cl]BF_4\cdot H_2O$